XL CILAMCE
IBERO-LATIN AMERICAN CONGRESS ON COMPUTATIONAL METHODS IN ENGINEERING
NOVEMBER 11-14, 2019
Praiamar Natal Hotel & Convention Natal, RN-BRAZIL

BAMBOO STRUT AND SISAL CABLE TENSEGRITY STRUCTURE FOOTBRIDGE

Nathalia B. de Albuquerque
Daniel C. T. Cardoso
nathalia.burger@gmail.com
dctcardoso@puc-rio.br
Department of Civil and Environmental Engineering, Pontifical Catholic University of Rio de Janeiro PUC-Rio
225 Marquês de São Vicente St., RJ 22451-900, Rio de Janeiro, Brazil
Mario Seixas
marioaseixas@puc-rio.br
Department of Arts & Design, Pontifical Catholic University of Rio de Janeiro PUC-Rio
225 Marquês de São Vicente St., RJ 22451-900, Rio de Janeiro, Brazil

Abstract. This paper presents a study on the behavior of a pedestrian bridge tensegrity structure built with natural materials. Initially, a prototype module of the structure is developed in a 1:25 scale. A constructive method is proposed applying foldable techniques for assembly and disassembly procedures. The methodology for the construction of the structure applied scaled models, from small to full-scale models. Bamboo culms of *Phyllostachys aurea* species were employed for the struts (compressive elements) and sisal ropes were selected for the cables (tensile elements). The modeling of the structure is carried out using the software Galileo, a program for structural analysis of tensegrity structures developed at PUC-Rio. Bar and cable elements were adopted to model the tensegrity footbridge. The effect of the prestress of the cables on the structure is studied. A comparison between the computational models considering a steel tensegrity structure and a bamboo strut and sisal cable net tensegrity structure with regard to the stresses acting on the cables and the displacement of the mid-span. Finally, the use of natural materials in civil engineering is evaluated regarding the mechanical performance of the structure.

Keywords: Tensegrity, Footbridge, Bamboo, Sisal, Modeling

1 Introduction

"A tensegrity is a system in a stable self-equilibrated state comprising a discontinuous set of compressed components inside a continuum of tensioned components" according to Prof. R.Motro [1]. Tensegrity structures were first designed by the artist K. Snelson in the 1940's [2, 3]. The terminology tensegrity was introduced by R.B. Fuller in the 60's as a contraction of the terms *tensile* and *integrity* [4]. This kind of structure has received notable interest among researchers of distinct disciplines such as architecture, biology, robotics, civil and aerospace engineering [5]. Tensegrity structures operate with two types of elements: cables – which bear tensile stresses – and struts – that sustain compressive stresses. Furthermore, they are classified as spatial, pin-jointed, lightweight and modular structures where stability and stiffness are obtained by a self-stress state of equilibrium, i.e., cables and struts are loaded by initial forces which provide a stable configuration for the system.

Additionally to their elegant appearance, tensegrity systems show good geometrical and structural efficiency, due to their considerable load-bearing capacity and intelligent employment of building materials. These characteristics draw the attention of structural designers and engineers [6] and current applications can be seen in domes, towers, roofs, temporary structures and exhibition pavilions [7]. In the field of bridges, some tensegrity structure propositions were made, such as the Passerella TorVergata in Rome, The Splash Bridge by Joel Cullum, and the National Building Museum Footbridge by Wilkinson Eyre and Arup in Washington DC, but few were actually built.

Designing a tensegrity structure can be a difficult assignment considering that it has not only a nonlinear behavior associated with the topology at hand, but also there is an absence of specific design guidelines for tensegrity structures. Many studies related to geometry and form-finding have been published, but few researches have focused on the design and construction of tensegrity structures.

The aim of this paper is to investigate the structural model for a tensegrity structure footbridge built with natural materials. A steel tensegrity pedestrian bridge and a bamboo and sisal tensegrity footbridge were computationally modeled, assuming a modular self-stressed structure. A comparison between the mechanical behavior of a steel structure and a bamboo structure is developed. A static analysis of vertical displacements and structural efficiency is studied using Newton-Raphson method. Finally, a construction method is proposed a bamboo strut and sisal cable net tensegrity footbridge.

2 Tensegrity footbridge

Barbarigos et al. [8] first presented the design of a tensegrity bridge in 2009. The structure consists of four individual tensegrity modules, each one spanning 5 m as shown in Fig. 1. The structural modules are based on a pentagonal prism containing fifteen nodes to outline three pentagonal layers. Fifteen struts are compressed by thirty cables connected on the top of the struts to form a modular tensegrity unit.

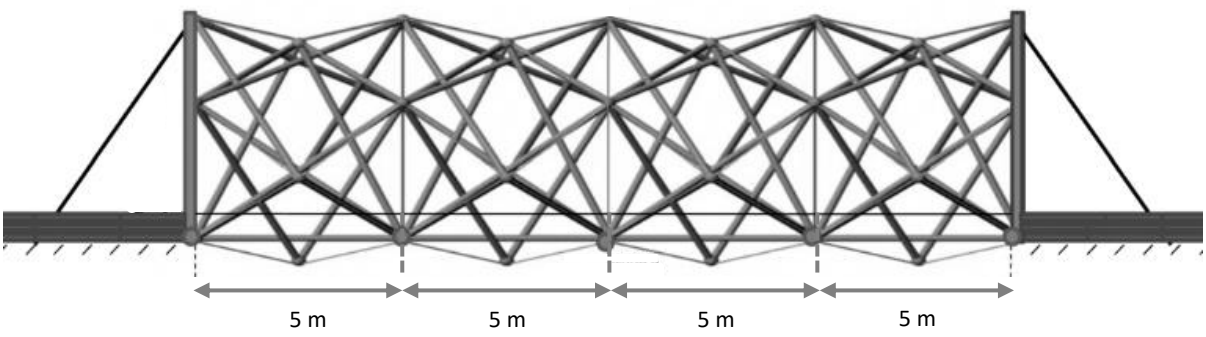

Figure 1 – Tensegrity footbridge (adapted from Barbarigos et al. [4])

Struts can be separated into two categories: (i) main struts and (ii) scissor struts. The first group depicts the five compressive members which bind the two outer pentagons, while the second group

portrays the ten elements linking the middle pentagon to the external ones. Likewise, the cables are classified based on their position: (i) ten layer cables form the two outlying pentagons and (ii) twenty x-cables link scissor struts nodes to outer pentagon nodes. Each individual module has a length of 500 cm in which main and scissor struts are 678 cm long, layer cables possess a length of 458 cm and x-cables have 347 cm in extent. The designed geometry ensures an adequate free space for pedestrian circulation.

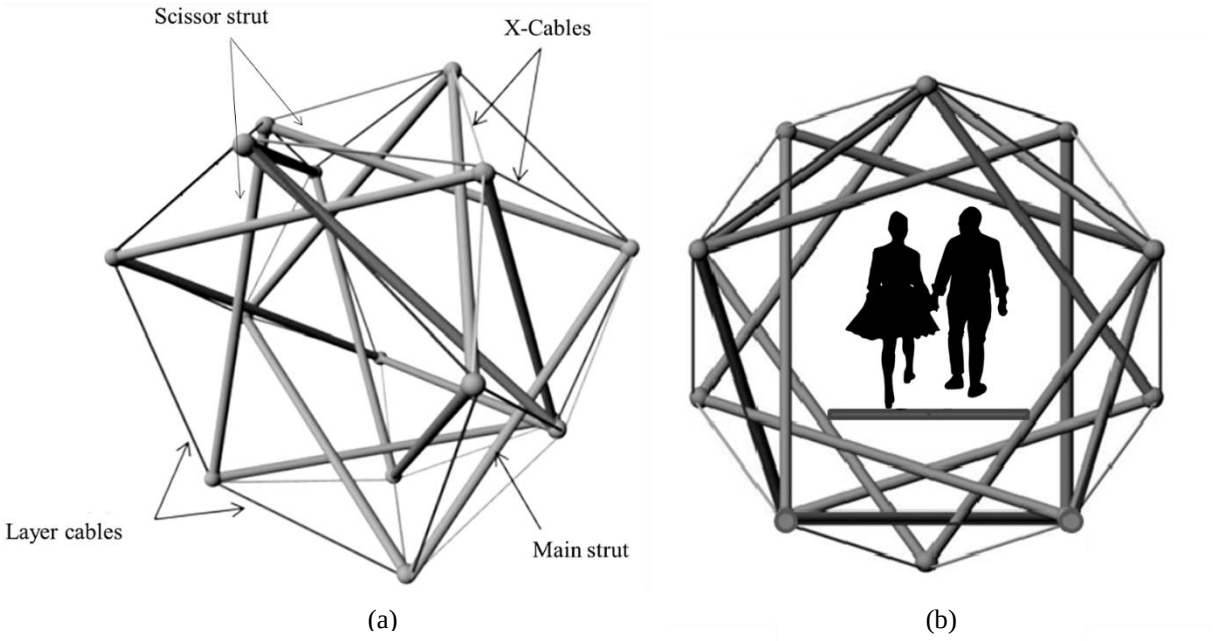

Figure 2 – Pentagon module: (a) isometric view and (b) cross section view (adapted from Korkmaz et al. [11])

It was considered for the structural model that the nodes at both extremities of the footbridge were fixed in all three translational directions as boundary conditions. Dead load was applied as nodal forces on the structure and live loads (vertical and horizontal) were applied on the four bottom nodes at each module.

The complete tables of node coordinates and node connectivity are presented below.

Table 1. Nodal coordinates

Node	x (cm)	y (cm)	z (cm)
1	0.00	0.00	389.40
2	0.00	370.30	120.30
3	0.00	228.90	-315.00
4	0.00	-228.90	-315.00
5	0.00	-370.30	120.30
6	250.00	0.00	-389.40
7	250.00	-370.30	-120.30
8	250.00	-228.90	315.00
9	250.00	228.90	315.00
10	250.00	370.30	-120.30
11	500.00	0.00	389.40
12	500.00	370.30	120.30
13	500.00	228.90	-315.00
14	500.00	-228.90	-315.00
15	500.00	-370.30	120.30

Table 2. Node connectivity

Element	Node	Node	Length (cm)	Type
1	1	2	458	Layer cable
2	2	3	458	Layer cable
3	3	4	458	Layer cable
4	4	5	458	Layer cable
5	5	1	458	Layer cable
6	11	12	458	Layer cable
7	12	13	458	Layer cable
8	13	14	458	Layer cable
9	14	15	458	Layer cable
10	15	11	458	Layer cable
11	1	9	347	X-cable
12	11	9	347	X-cable
13	2	9	347	X-cable
14	12	9	347	X-cable
15	2	10	347	X-cable
16	12	10	347	X-cable
17	3	10	347	X-cable
18	13	10	347	X-cable
19	3	6	347	X-cable
20	13	6	347	X-cable
21	4	6	347	X-cable
22	14	6	347	X-cable
23	4	7	347	X-cable
24	14	7	347	X-cable
25	5	7	347	X-cable
26	15	7	347	X-cable
27	5	8	347	X-cable
28	15	8	347	X-cable
29	1	8	347	X-cable
30	11	8	347	X-cable
31	1	12	678	Main strut
32	2	13	678	Main strut
33	3	14	678	Main strut
34	4	15	678	Main strut
35	5	11	678	Main strut
36	15	9	678	Scissor strut
37	9	3	678	Scissor strut
38	11	10	678	Scissor strut
39	10	4	678	Scissor strut
40	12	6	678	Scissor strut
41	6	5	678	Scissor strut
42	13	7	678	Scissor strut
43	7	1	678	Scissor strut
44	14	8	678	Scissor strut
45	8	2	678	Scissor strut

3 Computational models

Tensegrity structures present a nonlinear behavior when subjected to external forces and can experience large displacements even for small deformations. Ali et al. [9] stated that the self-stress is necessary for stabilizing the tensegrity structure by activating the geometrical stiffness. The equilibrium between tensile and compressive forces is responsible for the structural stability and load bearing capacity of tensegrity structures. Barbarigos et al. [8] also showed that structural properties and responses such as self-weight and deflection of the footbridge, respectively, are greatly influenced by different self-stresses applied on the structure. This demonstrates that the structural performance of tensegrity structures is very intricate and, therefore, different design parameters must be taken into consideration, such as material properties, cross-sectional areas of elements and levels of pretension.

The design of a tensegrity system can be investigated from the following aspects: (i) the form-finding process, (ii) the application of self-stress or (iii) the behavior under external loads. In this study, the scope of the work focused on the structural behavior under external loads. Static analyses of the tensegrities were performed using Galileo, a software developed by Dr. M. Santana at the Department of Civil and Environmental Engineering of PUC-Rio for structural analysis of deployable structures and tensegrities [10]. The software applies computational mechanics to simulate physical systems using numerical methods.

The following hypotheses are taken into consideration to formulate the model of the tensegrity footbridge:

- Cables and struts are straight and are concurrent in nodes;
- Elements are perfectly articulated at the nodes;
- Struts are designed as bar elements and, therefore, can absorb tensile or compressive forces;
- Cables can only carry tensile forces;
- External forces apply only to the nodes;
- Initial geometry and prestress conditions are previously established;
- Local and global buckling of struts are neglected;
- Incremental stiffness caused by external loads are disregarded.

Section 3 presents in detail the modeling of a steel tensegrity footbridge and bamboo and sisal tensegrity footbridge. The obtained results are presented for the both designed models.

3.1 Steel tensegrity footbridge

The steel tensegrity footbridge was modeled on Galileo using the configurations shown in Table 3. For the struts, steel grade S355 with an elasticity modulus of 210 GPa and yield stress of 250 MPa was used. For the cables, stainless steel with elasticity modulus of 115 GPa was chosen.

Table 3. Configuration for the steel tensegrity footbridge

Parameters	Value
Cable cross-section (cm²)	1.5
Cable elastic modulus (GPa)	115
Strut cross-section (cm²)	6.0
Strut elastic modulus (GPa)	210

Structural analyses were performed considering geometric nonlinearity. In this study, the static analysis of the tensegrity footbridge is performed using a modified Newton-Raphson iterative procedure. Table 4 presents the load combinations for the structure for the service limit-state according to Swiss SIA code [12,13]. For this study the wind loads were neglected.

Table 4. Design loads

Load	Safety factor	Value
Dead load	1.0	78.5 kN/m³
Vertical service load	1.0	4.0 kN/m²
Horizontal service load	1.0	10% of the vertical load

Vertical and horizontal service loads, initially acting on the surface of the deck, were applied as equivalent point loads on the four nodes of the tensegrity on which the deck is supported.

In addition to the design loads, the cables were also subjected to pretension. Prestress is a key aspect in tensegrity structures, since it garantees the stability and stiffness of the structure before external loads can be applied. In this study, prestress is specified as a percentage of the tensile strenght of the cable.

The deformed shape of the footbridge can be observed below. As expected, larger displacements can be observed at the mid-span of the structure. Fig. 3 shows the negative displacements of the structure in red (according to the blue Y axis in the center of the structure). The mermbers in blue presents positive displacements.

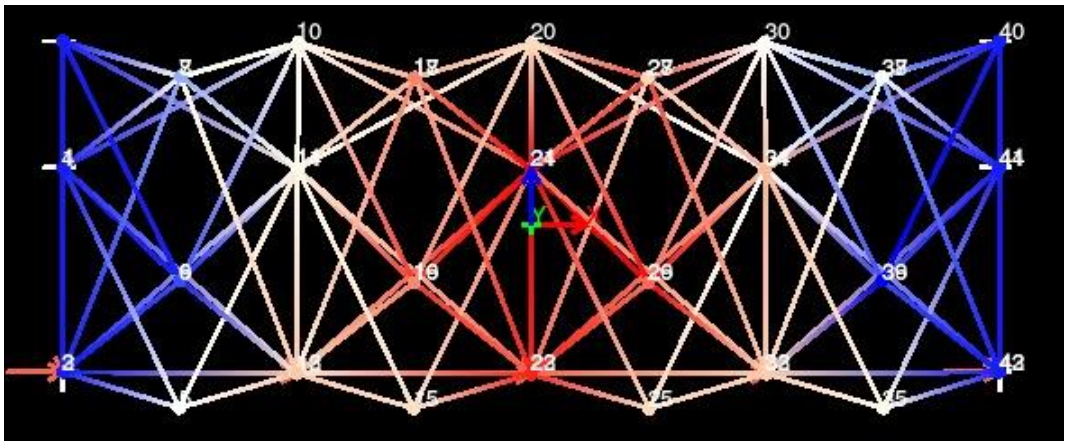

Figure 3 – Deformed steel tensegrity footbridge

Vertical displacements at the mid-span of the pedestrian bridge associated to different self-stress levels acting on the structure are shown in Fig. 4. It can be noted that overall self-stress and rigidity of the tensegrity model are directly proportional, i.e., increasing the self-stress applied on the model, the structure presented a better mechanical performance.

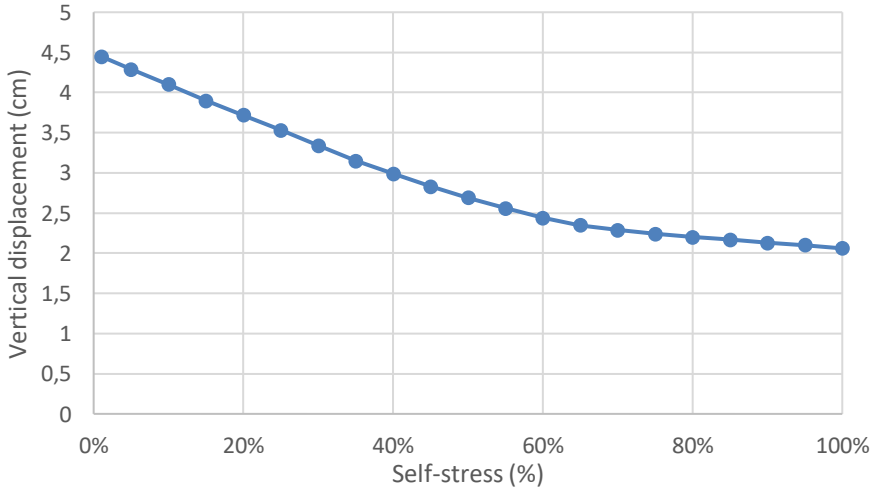

Figure 4 – Displacement vs. self-stress chart for the steel tensegrity footbridge

It can be observed that the results found above show reasonable agreement to those presented in [8]. Given a configuration in which cables have a 5% of self-stress in regard to their tensile strength, the model studied in this paper and the model proposed by Barbarigos et al. [8] presented similar values for maximum displacement as exhibited in Table 5.

Table 5. Vertical displacement at mid-span

Reference	Value
Galileo	4.3 cm
Barbarigos et al. [8]	4.2 cm

3.2 Bamboo strut and sisal cable tensegrity footbridge

The bamboo and sisal tensegrity footbridge was modeled in Galileo using the configurations shown in Table 6. For the struts, bamboo culms of *Phyllostachys aurea* species with an elasticity modulus of 12.5 GPa were used. For the cables, sisal rope with elasticity modulus of 30 GPa was chosen.

Table 6. Configuration for the bamboo strut and sisal cable tensegrity footbridge

Parameters	Value
Cable cross-section (cm²)	19.6
Cable elastic modulus (GPa)	30
Strut cross-section (cm²)	26.5
Strut elastic modulus (GPa)	12.5

The design loads applied were the same as the ones described in Table 4, adjusting solely the dead load. In order to meet serviceability limit-state requeriments, it was necessary to employ a bundled bamboo rod using three joined bars for each strut. Similarly to the steel tensegrity structure, larger displacements were observed at the mid-span of the structure (Fig. 5). It can be observed that, unlike the previous modeled steel structure, this structure shows small positive displacements, having mostly elements with negative or neutral displacements.

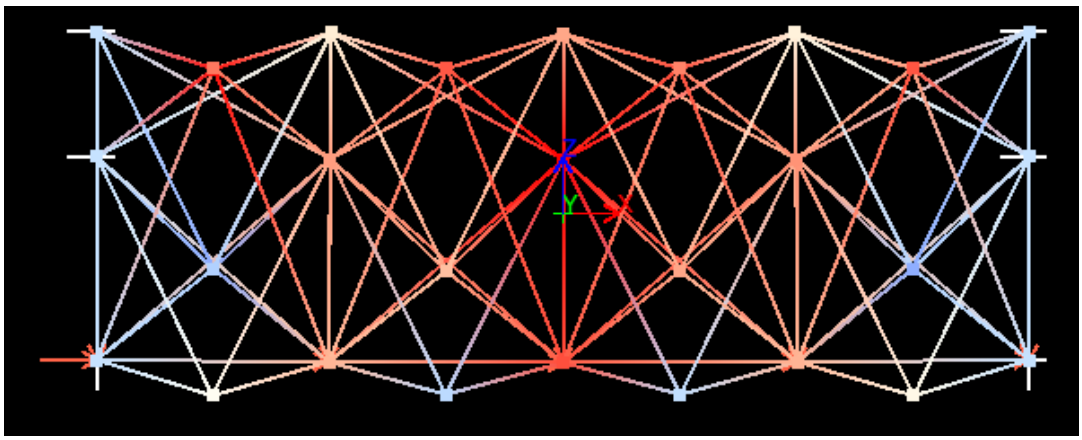

Figure 5 - Deformed bamboo and sisal tensegrity footbridge structure

As noticed in the steel structure, the bamboo and sisal tensegrity footbridge demonstrated good responses when subjected to increasing levels of prestress. The relation between vertical displacements at the mid-span and different self-stress levels acting on the structure are shown in Fig. 6.

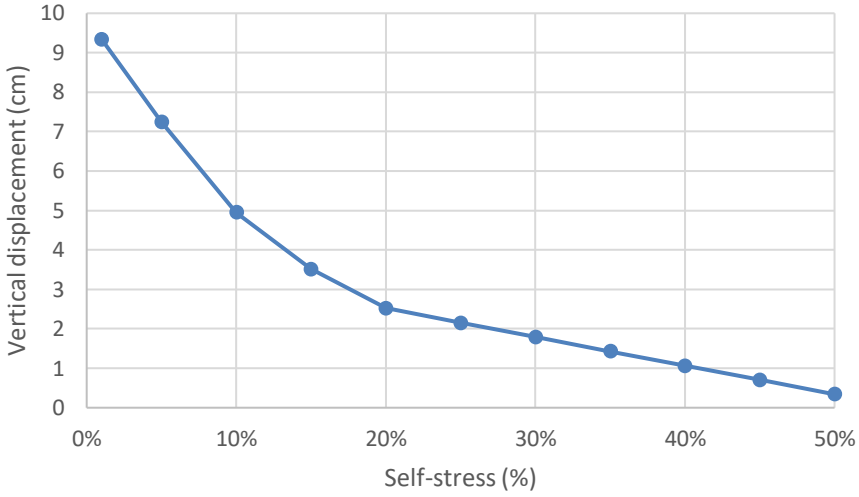

Figure 6 - Displacement vs. self-stress chart for bamboo and sisal tensegrity footbridge

At a 5% level of self-stress, the bamboo and sisal tensegrity structure presented a vertical displacement of 7.2 cm. The pretension demonstrated a great influence over the rigidity of the structure, especially from 0% to 20%, when vertical displacement decreased significantly.

3.3 Comparison of results

Based on the results shown previously, it is possible to assess the values obtained for vertical displacements for both steel tensegrity structure and bamboo and sisal structure tensegrity structure. Figure 7 shows how each bridge behaved under different self-stress levels. It can be noted that, initially, the bamboo and sisal tensegrity footbridge had a larger displacement at the mid-span of the structure. However, this structure demonstrated high sensitivity to prestress increment, becoming rapidly more rigid as self-stress was increased. On the other hand, the steel tensegrity footbridge revealed a low vertical displacement even for small prestresses and, even as the levels of self-stress increased, the structure showed little change.

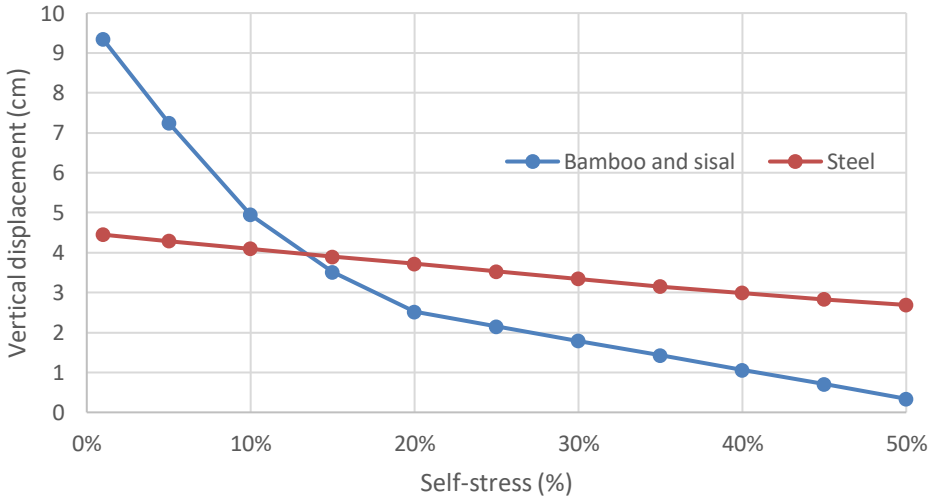

Figure 7 – Comparison of vertical displacements for steel tensegrity footbridge and bamboo and sisal tensegrity footbridge

Another parameter investigated in this study was the structural efficiency. A Structural Efficiency Index [8] was used to compare the steel tensegrity footbridge in contrast to the bamboo and sisal structure. The index is calculated as

$$\text{SEI} = \underbrace{\left(\frac{L+W}{W}\right)}_{\alpha} \times \underbrace{\left(\frac{S}{D}\right)}_{\beta} \times \underbrace{\left(\frac{L}{D}\right)}_{\gamma} \tag{1}$$

where L is the sum of design loads disregarding partial factors, W is the self-weight, S in the span of the bridge and D is the maximum displacement at mid-span.

The results presented in Table 7 show that the bamboo and sisal tensegrity footbridge is more structurally efficient than steel structure. Compared to the steel computational model, the bamboo and sisal structure demonstrated not only a better serviceability performance (β), but also an overall higher rigidity (γ). However, the steel tensegrity footbridge presented a better self-weight efficiency (α).

Table 7. Structural Efficiency Index

	$\frac{\alpha}{\alpha_{steel}}$	$\frac{\beta}{\beta_{steel}}$	$\frac{\gamma}{\gamma_{steel}}$	$\frac{SEI}{SEI_{steel}}$
Steel	1.00	1.00	1.00	1.00
Bamboo and sisal	0.80	1.12	1.21	1.09

4 Construction method

As discussed in section 4, it is structurally feasible to enterprise a tensegrity footbridge using natural materials such as bamboo and sisal. Therefore, a construction method is proposed in the present study to enable the construction of such structure. The steps to build a small bamboo and sisal scale model are listed below.

- Step 1: *Mise en place*

The miniature model was first separated by element types – main struts, scissor struts, layer cables and x-cables – and then color-coded. The five layer cables which compose the inferior pentagon were colored in yellow. Similarly, the five layer cables that form the superior pentagon were colored in green. Ten red cables connect scissor strut nodes to the lower pentagon and ten blue cables connect the same nodes to the upper pentagon. The main struts were colored in black and scissor struts were colored in white.

- Step 2: Initial set up

The construction method starts by disposing the black main struts and the yellow layer cables on the surface to create a regular pentagon, as shown in Fig. 8a. At the same time, scissor struts are assembled together with two red x-cables and two blue x-cables (Fig. 8b).

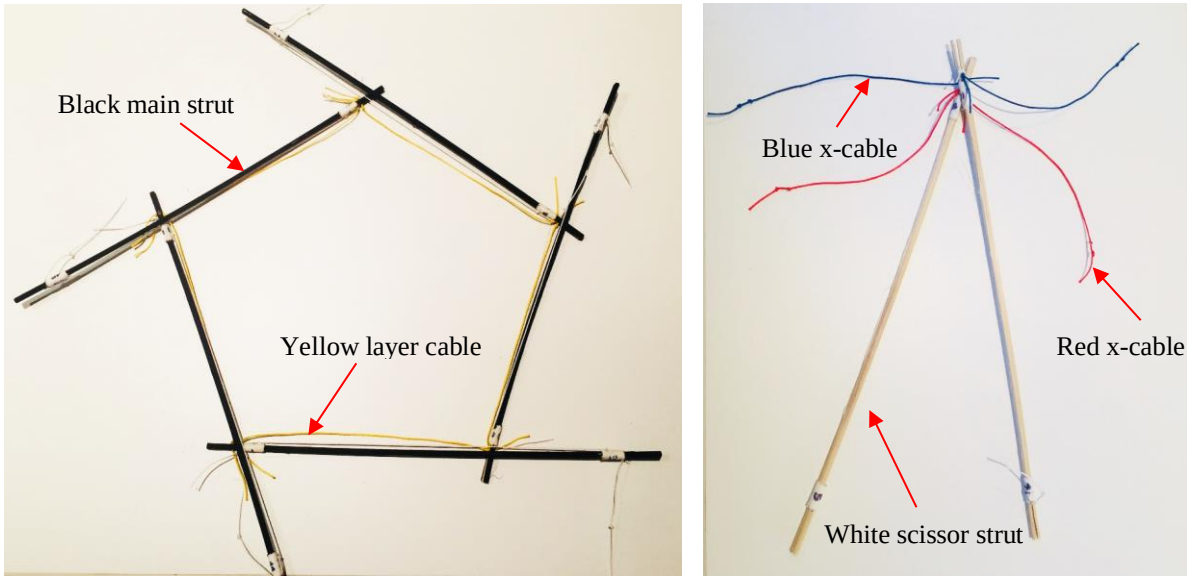

(a) **(b)**

Figure 8 - Initial steps to build a small scale bamboo and sisal tensegrity structure: laying out the (a) main struts connected to inferior layer cables and (b) the scissor struts connected to x-cables

- Step 3: Tessellation of struts and cables

After the initial set up, displayed on Fig. 8a, each scissor is consecutively inserted at the midpoint of line segments $\overline{1,2}$, $\overline{2,3}$, $\overline{3,4}$, $\overline{4,5}$ and $\overline{5,1}$, respectively. Next, lower and upper x-cables are connected to the adjoining main struts. The detailed step-by-step of these stages are shown below.

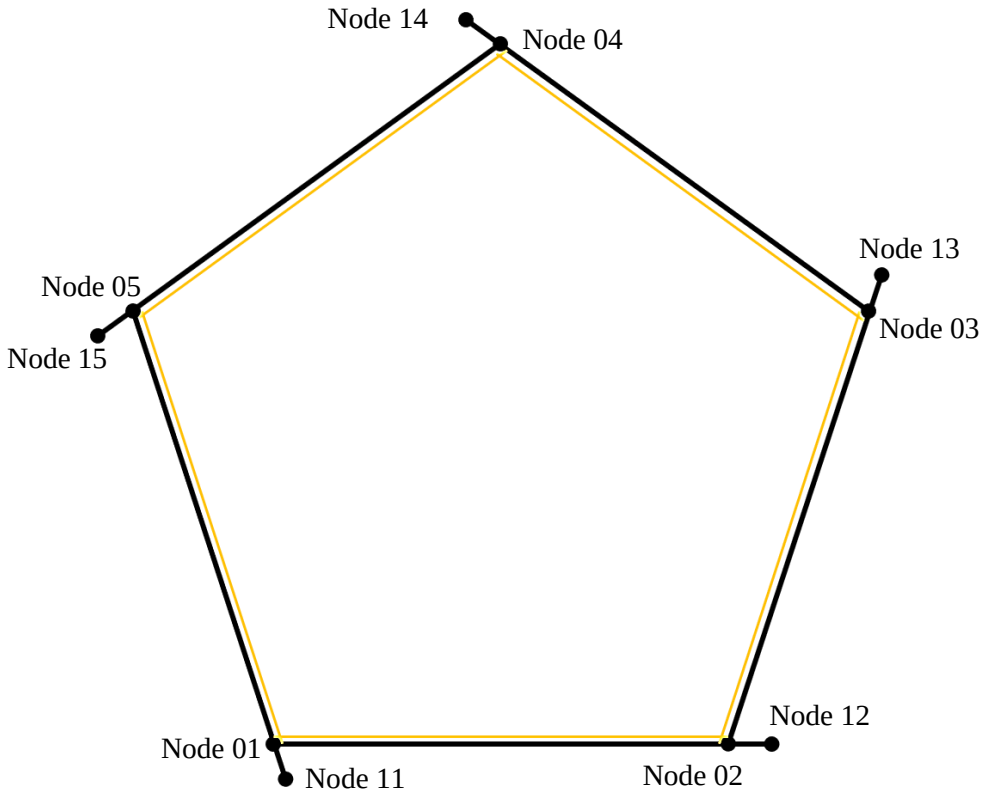

Figure 9 – Connection of the main struts with the inferior layer cables

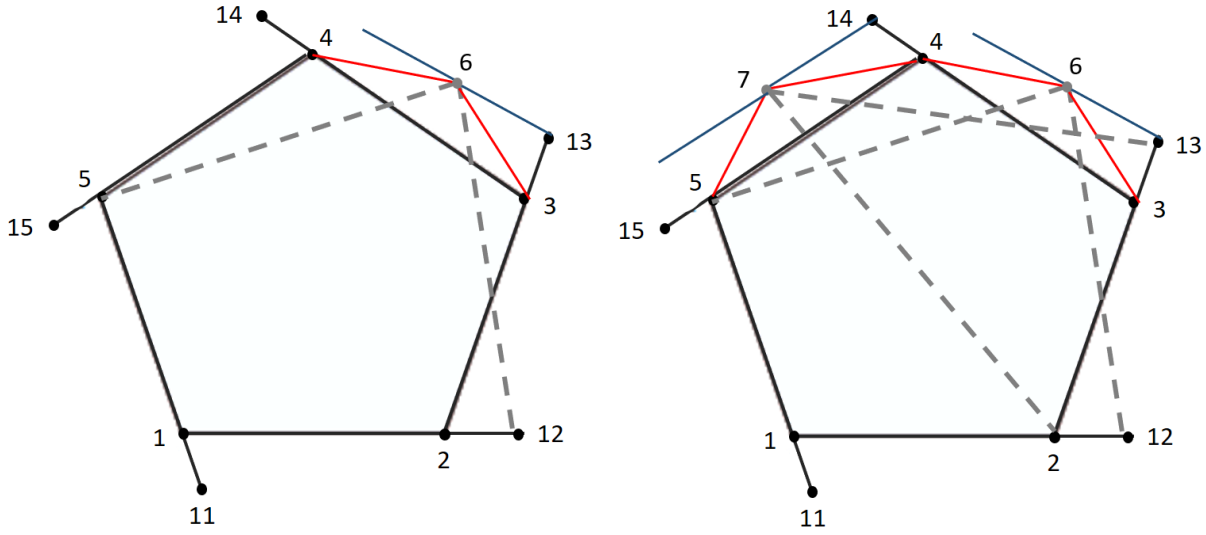

(a) **(b)**

Figure 10: (a) Connection of the first scissor, node 6, and (b) connection of the second scissor, node 7

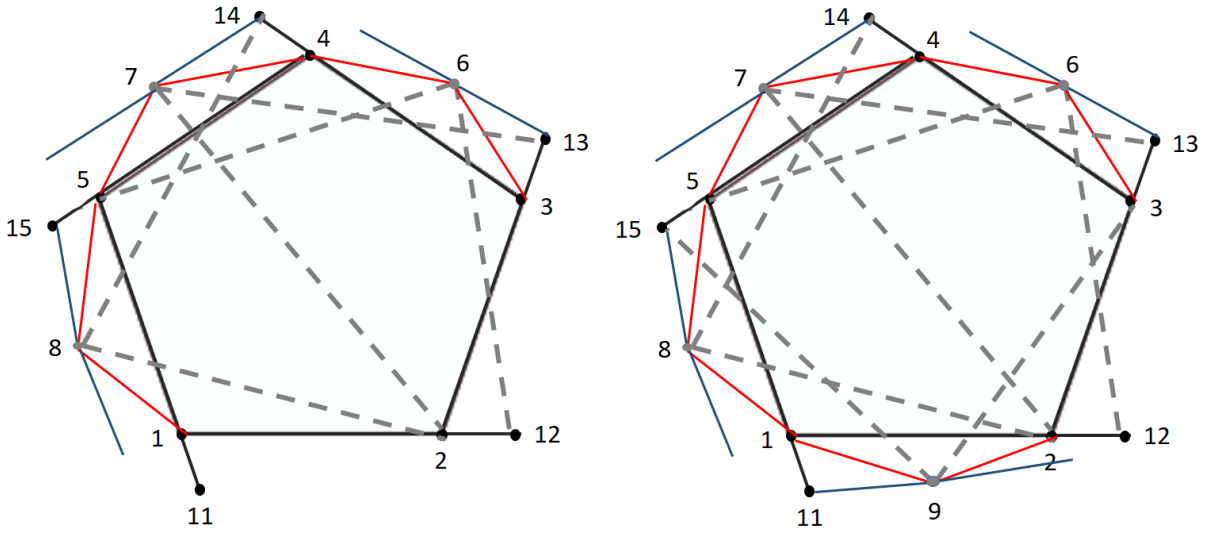

(c) **(d)**

Figure 10: (c) Connection of the third scissor, node 8, and (d) connection of the fourth scissor, node 9

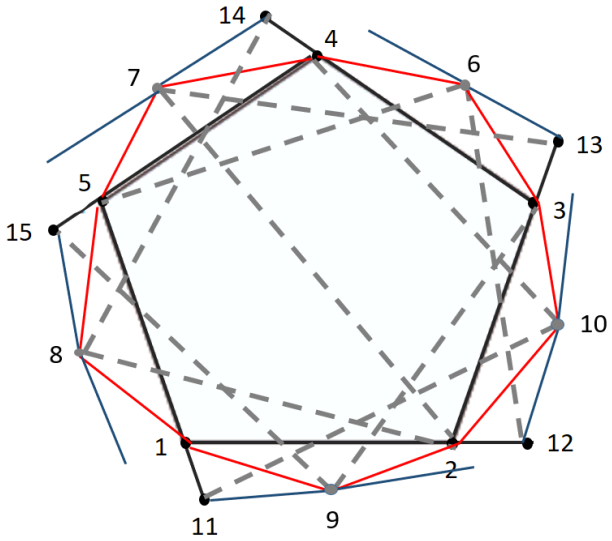

(e)

Figure 10: (e) Connection of the fifth and final scissor, node 10

- Step 3: Elevation

Once the module is laid out on the ground, as seen in Fig. 10e, a mast is set at the center of the pentagon. Five temporary cables connect nodes 11, 12, 13, 14 and 15 to the top of the pole. Pulleys are used to raise the structure. When all constrained x-cables reach their full length, i.e., there is no slacking, the loose ends of the unconstrained x-cables are fixed to the nodes of the superior pentagon. Finally, each green layer cable is put into place individually.

As the final green cable is secured, the tensegrity structure presents a stable behavior. Figure 11 presents the finished small scale tensegrity module. At this stage, external loads can be applied on the module.

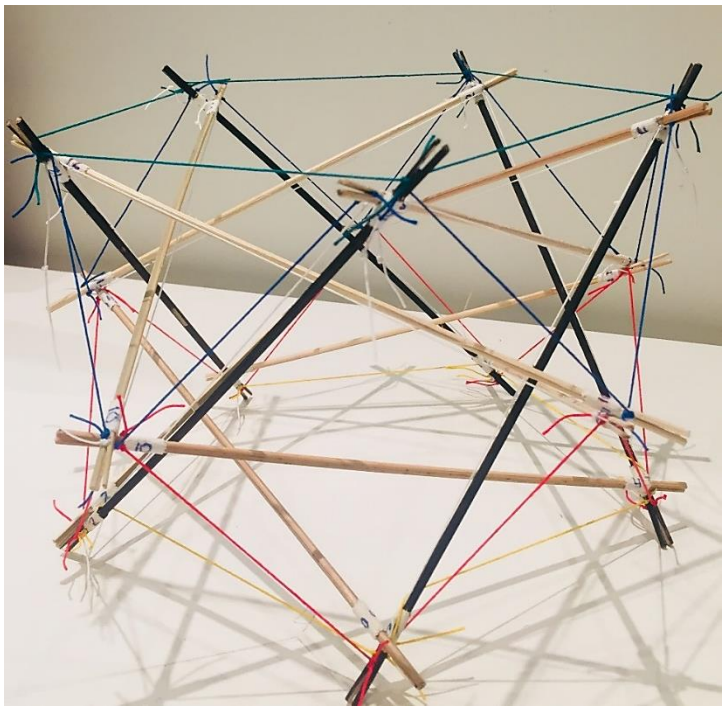

Figure 11 – Final form of the tensegrity module

5 Conclusions

A tensegrity structure footbridge was presented in this paper. It was designed two computational models: the first model used steel elements for struts and cables, whereas the second one used natural materials, such as bamboo for the struts and sisal for the cable nets. A static analysis was carried out in both models to understand the behavior of each structure with respect to pretension and vertical displacement. Then, a comparison between the structural behavior of the computer models in steel and bamboo and sisal was studied. This work results in the following conclusions:

- The steel tensegrity footbridge modeled using Galileo, a novel software for structural analysis of tensegrity structures, showed good concordance to the values presented in [8]. The software was considered an adequate tool for modeling such steel structure.
- The bamboo strut and sisal cable tensegrity structure demonstrated great potential for structural engineering as the modeled structure presented a higher structural efficiency index when compared to the steel tensegrity structure model.
- A construction method has been developed with sustainable and low environmental impact techniques, using craftsman handmade processes. The construction techniques were accessible and can be disseminated in regions of the globe with limited resources.

Acknowledgements

Authors would like to thank Dr. Murillo Santana and the Department of Civil and Environmental Engineering of Pontifical Catholic University of Rio de Janeiro for supporting this work.

References

[1] R. Motro. *Tensegrity: structural systems for the future*. Penton Science; 2003.

[2] K. Snelson. The art of Tensegrity. *International Journal of Space Structures*, vol. 27, n. 2 & 3, pp. 70-80, 2012.

[3] K. Snelson. *Continuous tension, discontinuous compression structures*, US Patent 3169611, 1965.

[4] R.B. Fuller. *Synergetics: explorations in the geometry thinking*. Nova York: Macmillian Publishing Company, 1982.

[5] R. E. Skelton and M. C. de Oliveira. *Tensegrity systems*, Springer, 2009.

[6] C. Plescan, M. Contiu and A. Dósa. A study of a tensegrity structure for a footbridge. *Third China-Romania Science and Technology Seminar (CRSTS 2018).*

[7] G. Victor, M. Seixas, J.L.M. Ripper. Estruturas Autoportantes Biotensegrity Aplicando Materiais Naturais. *In: Métodos e Processos em Biônica e Biomimética: a Revolução Tecnológica pela Natureza*, pp. 152 -171. Blucher, 2018.

[8] L. Rhode-Barbarigos, N. B. H. Ali, R. Motro and I. F. C. Smith. Designing tensegrity modules for pedestrian bridges. *Engineering Structures*, vol. 32, pp. 1158-1167, 2009.

[9] N. B. H. Ali, L. Rhode-Barbarigos, A. A. P. Albi and I. F. C. Smith. Design optimization and dynamic analysis of a Tensegrity-based footbridge. *Engineering Structures*, vol. 32, pp. 3650-3659, 2010.

[10] M. V. B. Santana. Tailored Corotational Formulations for the Nonlinear Static and Dynamic Analysis of Bistable Structures. PhD thesis, Université Libre de Bruxelles & Pontifical Catholic University of Rio de Janeiro, 2019.

[11] S. Korkmaz, N. B. H. Ali and I. F. C. Smith. Configuration of control system for damage tolerance of a tensegrity bridge. *Advanced Engineering Informatics*, vol. 26, pp. 145-155, 2012.

[12] SIA 260 — Basis of structural design: swiss society of engineers and architects. Zurich, 2003.

[13] SIA 263 — Steel construction: swiss society of engineers and architects. Zurich, 2003.